Title

Aging differentially affects LTCC function in hippocampal CA1 and piriform cortex pyramidal neurons

Permalink

https://escholarship.org/uc/item/4xw837mc

Journal

Cerebral Cortex, 33(4)

ISSN

1047-3211

Authors

Maziar, Aida

Critch, Tristian NRHY

Ghosh, Sourav

et al.

Publication Date

2023-02-07

DOI

10.1093/cercor/bhac152

Peer reviewed

OXFORD

Aging differentially affects LTCC function in hippocampal CA1 and piriform cortex pyramidal neurons

Aida Maziar, MSc[1,†], Tristian N.R.H.Y. Critch, MSc[1,†], Sourav Ghosh, PhD[1,†], Vishaal Rajani, PhD[1,†], Cassandra M. Flynn, MSc[1],

Tian Qin, BSc[1], Camila Reinhardt, BSc[1], Kwun Nok Mimi Man, PhD[2], Amy Lee, PhD[3], Johannes W. Hell, PhD[2], Qi Yuan (ID), PhD[1,*]

[1]Division of Biomedical Sciences, Faculty of Medicine, Memorial University, St. John's, NL A1B 3V6, Canada,
[2]Department of Pharmacology, School of Medicine, University of California-Davis, Sacramento, CA 95817, United States,
[3]Department of Neuroscience, University of Texas-Austin, Austin, TX 78712, United States
*Corresponding author: Biomedical Sciences, Faculty of Medicine, Memorial University, St. John's, NL A1B 3V6, Canada. Email: qi.yuan@med.mun.ca

[†]Equal contributions.

Aging is associated with cognitive decline and memory loss in humans. In rats, aging-associated neuronal excitability changes and impairments in learning have been extensively studied in the hippocampus. Here, we investigated the roles of L-type calcium channels (LTCCs) in the rat piriform cortex (PC), in comparison with those of the hippocampus. We employed spatial and olfactory tasks that involve the hippocampus and PC. LTCC blocker nimodipine administration impaired spontaneous location recognition in adult rats (6–9 months). However, the same blocker rescued the spatial learning deficiency in aged rats (19–23 months). In an odor-associative learning task, infusions of nimodipine into either the PC or dorsal CA1 impaired the ability of adult rats to learn a positive odor association. Again, in contrast, nimodipine rescued odor associative learning in aged rats. Aged CA1 neurons had higher somatic expression of LTCC Cav1.2 subunits, exhibited larger afterhyperpolarization (AHP) and lower excitability compared with adult neurons. In contrast, PC neurons from aged rats showed higher excitability and no difference in AHP. Cav1.2 expression was similar in adult and aged PC somata, but relatively higher in PSD95− puncta in aged dendrites. Our data suggest unique features of aging-associated changes in LTCCs in the PC and hippocampus.

Key words: aging; hippocampus; L-type calcium channels; piriform cortex.

Introduction

A primary tenet of modern neuroscience is that calcium is a central mediator of brain signaling. Specific patterns of elevated intracellular calcium are essential for initiating signaling cascades that lead to long-term synaptic plasticity underlying learning and memory formation. However, aging is associated with rises in intracellular calcium levels, which can lead to calcium dysregulation, contributing to age-related cognitive dysfunction and memory loss. A "calcium hypothesis" of brain aging was proposed in the 1980s (Khachaturian 1984; Landfield 1987; Khachaturian 1989; Porter et al. 1997) and a central component of the calcium aging hypothesis is age-related hyperfunction of L-type calcium channels (LTCCs). Hippocampal CA1 pyramidal neurons of aging animals display overexpression of LTCCs (Thibault and Landfield 1996; Nunez-Santana et al. 2014; Zanos et al. 2015), increased LTCC phosphorylation (Davare and Hell 2003) and channel conductance (Campbell et al. 1996; Disterhoft et al. 2004). Hyperfunction of LTCCs is also associated with increased afterhyperpolarization (AHP; Landfield and Pitler 1984; Power et al. 2002) and reduced

neuronal excitability in the hippocampus (Disterhoft et al. 1996). Despite the important role of LTCCs in synaptic plasticity in adult animals, reducing LTCC activities in aged human or animals have been shown to paradoxically enhance cognitive function and various types of learning. Blocking LTCCs with nimodipine or isradipine results in increased excitability of aging CA1 pyramidal cells (Thompson et al. 1990; Moyer Jr et al. 1992) and facilitates associative learning in aging rabbits (Deyo et al. 1989), rats (Levere and Walker 1992; Batuecas et al. 1998; Veng et al. 2003; Hopp et al. 2014) and monkeys (Sandin et al. 1990). In humans, some beneficial results of nimodipine on cognition have been reported in patients with various types of dementia (Ban et al. 1990; Tollefson 1990; Sze et al. 1998; Lopez-Arrieta and Birks 2002; Wang et al. 2006). Whether LTCC hyperfunction and learning enhancement by LTCC blockade, are general features of the aging brain or are unique to the hippocampus is not well known.

The piriform cortex (PC) is the primary olfactory cortex involved in odor perception, discrimination, and associative memories (Barkai and Saar 2001;

Wilson and Sullivan 2011; Ross and Fletcher 2019). Decreased olfactory function is common in aging populations and is an early warning sign for Alzheimer's disease (AD; Murphy 1999; Wilson et al. 2009). Disruption of central olfactory processing in the PC has been identified as an important mediator for olfactory deficiency in AD in both humans and rodent models (Li et al. 2010; Wesson et al. 2011a, 2011b; Wilson et al. 2014; Ghosh et al. 2019). PC and hippocampus have intensive mutual connections and coordinate in contextual, spatial, and olfactory learning (Truchet et al. 2002; Zelcer et al. 2006; Zhang and Manahan-Vaughan 2015; Rangel et al. 2016; Strauch and Manahan-Vaughan 2020; Poo et al. 2021). Both PC and hippocampus-related cognitive functions are sensitive to aging. Olfactory recollection deficiency is correlated with spatial memory impairment in rodent aging models (Eichenbaum and Robitsek 2009). However, aging-associated neuronal changes in the PC have not been extensively studied. Although LTCCs in the PC have a critical role in synaptic plasticity and odor associative learning in neonate rodents (Mukherjee and Yuan 2016; Ghosh et al. 2017a, 2017b), the contributing role and molecular underpinnings of the PC LTCCs in adult and aging animals have not been explored.

In this work, we explore age-dependent changes in spatial and olfactory functions associated with the hippocampus and PC. We compare LTCC subunit expression and neuronal properties in pyramidal neurons of hippocampus and PC. Our results reveal differential age-dependent LTCC expression and function in the 2 structures. LTCC hyperfunction-associated hypo-excitability was not a feature of neurons in aged PC, although earlier findings in the hippocampus were replicated. We suggest that memory encoding systems have varying vulnerability with age and that aging-associated changes in LTCC substrates depend on neuronal context.

Materials and methods
Subjects
Adult or aged Sprague–Dawley rats of mixed sexes were used. Rats were kept in a standard 12-h light–dark cycle, with food and water ad libitum. For behavioral experiments, 6–9 and 19–23-month-old rats were used. For immunohistochemistry (IHC), western blotting (WB) and electrophysiological recording, 3–6 and 19–25-month-old rats were used. Experimental procedures were approved by the Institutional Animal Care Committee at Memorial University of Newfoundland and followed Canadian Council's guidelines on Animal Care.

Experimental design and statistical analysis
This work characterized age-dependent expression and functions of LTCCs in the PC, in comparison with CA1 age-dependent LTCC alterations that have been previously characterized. Behavioral experiments probed LTCC dependency in spatial and olfactory learning. Three behavioral experiments were explored: (i) a spontaneous

location recognition test that is dependent on the hippocampal function (Bekinschtein et al. 2013); (ii) a similar odor discrimination test that is mediated by the PC (Xu et al. 2014); and (iii) an associative odor learning paradigm in which both the hippocampal CA1 and PC are critically involved (Zelcer et al. 2006). Both sexes were used in behavioral experiments. LTCC cellular expressions were measured by IHC and WB. LTCC modulation of neuronal excitability in the PC and CA1 was measured by whole cell recording. One to 3 recordings from each brain (one cell per slice) were used for analysis. Sample numbers in the behavioral, IHC and WB experiments are the numbers of animals used. Sample numbers in the electrophysiological experiments are the numbers of the cells recorded.

OriginPro 9.0 software was used to analyze all data. Data were reported as the mean ± SEM. For group comparisons in behavioral experiments in Fig. 1, 2-way (treatment × age) analyses of variance (ANOVAs) were used, followed by post-hoc Tukey tests. Odor associative learning in Fig. 2 was measured by 1-way (memory duration) or 2-way (learning time course × group) repeated ANOVAs, followed by Tukey tests. Two group comparisons in Figs 3–6 and Tables 1 and 2 used unpaired *t*-tests. Two-way repeated ANOVAs were used to compare excitability differences in the input/output (I/O) curves of currents vs. action potential (AP) numbers in Fig. 6. Differences between groups were considered significant when *P* values were <0.05.

Cannula surgery
Rats were anesthetized using Isoflurane and then mounted in a stereotaxic apparatus and placed in the skull flat position. The holes for the cannulas were drilled for PC (AP: −2.3 and ML: ± 5.4) or for CA1 (AP: −3.6 and ML: ± 2.6). The cannulas were lowered into place (DV: 8.9 for PC and 2.2 for CA1, respectively) from the brain surface, and then affixed to the skull via dental cement. The incisions were sutured and rats were put back to their cages for recovery. A subset of rats was perfused following the behavioral experiments for checking targeting placement (Supplementary Fig. 1).

Behavioral experiment
Spontaneous location recognition task
Rats were placed in an open arena (60 × 60 × 40.5 cm³) for 10 min with 3 identical objects (1, 2, and 3) placed at specific positions. Object 1 was placed on one side and Objects 2 and 3 were placed on the opposite side of the arena, 20 cm apart from each other. During testing (24 h later), rats were placed in the same arena with 2 identical objects, one in the same position as Object 1 (a familiar location, F), the other midway between the previous Objects 2 and 3 (a novel location, N). The discrimination ratio was the difference between time spent at the novel and familiar objects over the total time spent on both objects (($t_{novel} − t_{familial})/t_{total}$) (Bekinschtein et al. 2013).

Similar odor discrimination

Rats were presented with a series of odors, delivered using a perforated micro-centrifuge tube containing 60 μL of odorant or mineral oil. The sequence was 3 trials of mineral oil, 3 trials of odor 1 (O1, 1-heptanol, 0.001%), and one trial of odor 2 (O2, 1-heptanol and 1-octanol in a 1:1 ratio, 0.001%). Each trial lasted 50 s and the inter-trial interval was 5 min. The tests were videotaped and sniffing time within a 1-cm radius around the odor tube was measured. The discrimination index was the ratio of the sniffing time difference between the O2 and the 3rd presentation of O1 to the total sniffing time $(t_{O2} - t_{O1-3})/(t_{O2} + t_{O1-3})$.

Odor associative learning

Rats were food deprived for 3–6 days before the onset of the experiments and food deprivation continued during the course of the experiment. Rats were placed in an open arena ($60 \times 60 \times 40.5$ cm^3) with 2 scented sponges, in a dimly lit room. Reese's puff cereal was used as a food reward. Rats learned to discriminate between 2 scented sponges in order to retrieve the food. Cereal pellets were placed in a retrievable center hole in one scented sponge, and placed in a hidden hole in the other scented sponge. This procedure consisted of a habituation phase, followed by an associative training phase. In the habituation phase, rats were exposed to an unscented sponge placed in random locations, baited with food. This is repeated for 4–10 days until the rats learned the task of retrieving food from the sponge.

In the associative training phase, rats were placed in a designated home corner and presented with 2 scented sponges (locations varied each trial randomly) and they were given a maximum of 300 s to retrieve the cereal pellet. Trials ended as soon as the animal retrieved the food. The total number of nose pokes the animal made on either sponge was recorded during each trial. Percentage of correct responses was counted as the number of correct responses over the number of total nose pokes. A subset of the rats was trained by a blind experimenter and similar results were yielded. Data were pooled from all rats trained.

Odor memory tests were carried out at either 3- or 6-week following training. Rats were placed in the same apparatus with 2 scented sponges (no food was present during this task) for 300 s as in the training sessions. The percentage of nose pokes over the previously rewarded scented sponge was measured during the memory test.

Drug administration

Drugs or vehicle were given either by i.p. (nimodipine, 5.5 mg/kg) or infused in the brain (100 μM; 0.5 μL per site; dissolved in 25% DMSO and 75% PBS) 30 min before training via a 10-μL Hamilton syringe and infusion pump. Similar dose of systemic injections of nimodipine have been used in rabbits and rats (Woodruff-Pak et al. 1997; Chakrabarti et al. 1998; Michaluk et al. 1998), with little effect on cardiovascular response (Chakrabarti et al. 1998; Michaluk et al. 1998). The infusion dose was chosen based on in vitro data of nearly complete blockade of both Cav1.2 and Cav1.3 subunits with 10-μM nimodipine (Xu et al. 2014). A higher dose (100 μM) was chosen for infusion to ensure efficient blockade of channel activity in vivo. The infusion was done over 3 min followed by 1 min wait before withdrawing the syringe.

Immunohistochemistry

Rats were perfused transcardially with ice-cold saline (0.9%), followed by 4% paraformaldehyde (PFA) in a 0.1 M phosphate buffer. Brains were collected and stored in 4% PFA for 24 h at 4°C and then transferred to a 0.1-M phosphate buffered saline (PBS). Fifty μm coronal sections were cut using a vibratome (Leica VT 1000S, Concord, ON, or Compresstome VF-310-OZ, Greenville, NC), and transferred to 24 well plates containing PVP. Free-floating sections were stored at 4°C until further processing.

For single antibody fluorescence staining, sections were washed 3×5 min in Tris buffer (0.1 M, pH 7.6) to remove the remaining PVP solution. Each section was then blocked in 1 mL 5% bovine serum albumin (BSA) in Tris buffer for 1 h at room temperature on a shaker. Sections were then incubated with a primary antibody (FP1 rabbit anti-Cav1.2 antibody (1:2,000) (Buonarati et al. 2017) in 5% BSA in Tris buffer on shaker at 4°C overnight. Sections were then washed 3×10 min in Tris buffer and probed with anti-rabbit secondary antibody Alexa 647 (1:500; Thermo Fisher Scientific, Mississauga, ON) in 5% BSA in Tris buffer for 1 h. Nuclei were counterstained with 4′-6-diamidino-2-phenylindole (DAPI; Abcam, Cambridge, UK) and slides were cover slipped.

For double antibody fluorescence staining, after completing the staining for the first antibody (Cav1.2 FP1), sections were washed 3×5 min in Tris buffer followed by 1×10 min wash in Tris A (0.1% Triton-X-100 in Tris buffer) and 1×10 min wash in Tris B (0.1% Triton-X-100 and 0.005% BSA in Tris buffer). Thereafter the sections were incubated with mouse anti-PSD-95 antibody (1:2,000; Invitrogen, Burlington, ON) in 5% BSA in Tris B on shaker at 4°C overnight. Sections were washed 1×10 min in Tris A followed by 1×10 min in Tris B. They were probed with anti-mouse secondary antibody Alexa 488 (1:500; Thermo Fisher Scientific, Mississauga, ON) in 5% BSA in Tris B for 1 h on a shaker. Sections were then washed 3×5 min in Tris buffer and mounted on chrome-gelatin coated slides. Slides were covered slipped and kept at 4°C before confocal microscopy scanning.

Fluorescence microscope, confocal scanning, and image analysis

For single antibody labeling, images were obtained with an EVOS M5000 microscope (Thermo Fisher Scientific, Mississauga, ON), from 4 to 5 sections cross rostral to caudal range. Images were taken from the dendritic and somatic layers of dorsal hippocampus (CA1, CA3, and

DG) and PC at a magnification of 20×. The intensity of light and exposure parameters was standardized across all captured images. Image analysis was performed using ImageJ software. In hippocampal CA1, CA3 and DG, and PC, regions of interest (ROI) were drawn in both dendritic and somatic layers. For each ROI, the integrated fluorescent intensity (normalized to the ROI area) was calculated. Fluorescence intensity of all slices of each animal was averaged.

Confocal imaging for fluorescence double labeling was conducted with an FV10i confocal microscope (Olympus). Z-stacks (~0.4 mm^2) were taken from the dendritic layer of dorsal hippocampus (CA1, CA3, and DG) and PC layer Ia and lb (averaged for PC dendritic layer) at a magnification of 60× with a 10× zoom. Z-stacks were acquired from 3 to 4 sections from rostral to caudal area. Photomultiplier tube assignments, confocal aperture size, and contrast remained constant for all sections.

Otsu method in image thresholding was used to perform automatic image segmentation into foreground and background. Using Grana's (BBDT) algorithm, connected components were identified. In order to remove noise of images, 2 filters of size 11 × 11 and 5 × 5 were applied resulting in creating 2 masks. Using the logical 'AND' operator between these 2 masks identified regions of overlap between 2 channels. Next, by using Grana's (BBDT) again, the overlapped regions of 2 images were counted.

Whole-cell tissue extraction and WB

Rats were anesthetized using isoflurane and decapitated. PC and hippocampus were collected and flash frozen on dry ice. Samples were stored at −80°C until further processing. For whole cell extraction, tissue was homogenized in ice-cold RIPA buffer (400 μL), containing inhibitor cocktail and phosphatase inhibitor cocktail (Roche). This suspension was vortexed and incubated at 4°C for 30 min with gentle rotation and then centrifuged at 13,500 rpm at 4°C for 15 min. The clear lysate supernatant was collected and stored at −80°C until further processing.

Total protein concentration was quantified by standard Pierce$_{TM}$ BCA assay (Thermo Fisher Scientific, Mississauga, ON). Equal amounts of protein (25 μg/μL for whole-cell, 40 μg/μL for extrasynaptic, and 10 μg/μL for synaptic fraction), sample buffer (0.3-M Tris–HCl, 10% SDS, 50% glycerol, 0.25% bromophenol blue, and 0.5-M dithiothreitol), and dH2O were prepared and boiled at 100°C for 2 min.

Samples were loaded in 7% SDS-PAGE gel, along with a protein ladder (Thermo Scientific, Mississauga, ON). The gels were then transferred to nitrocellulose membranes (0.45 μm; Thermo Fisher Scientific). The membranes were stained with reversible Ponceau S staining and scanned at 600 dpi to a TIFF file using a standard scanner. After that, the membranes were rinsed in 1X TBST for 10–15 min until the staining was completely eliminated. The membranes were blocked for 2 h with 5% non-fat dry milk at room temperature, then incubated at 4°C overnight with an Ab144 rabbit anti-Cav1.3 (1:1,000) antibody (Nunez-Santana et al. 2014). Next day membranes were washed 3 × 5 min with 1X TBST. Anti-rabbit HRP-bounded second antibody was applied (1:10,000; Thermo Scientific, Mississauga, ON) at room temperature for 1.5 h within 1X TBST and then washed 3 × 10 min in 1X TBST.

The protein bands were visualized using chemiluminescent substrate (Thermo Fisher Scientific, Mississauga, ON) and the optical density (OD) of each band was measured using ImageJ software and normalized to Ponceau staining of corresponding total protein density.

Electrophysiological recordings

Slice preparation of hippocampus and piriform cortex

Rats were anesthetized with pentobarbital (150 mg/kg) and then decapitated for brain extraction. Parasagittal slices (300 μm) were obtained with a vibratome (Leica 1200S, Concord, ON). To preserve the health of slices from aging animals, rats were intracardially perfused with ice-cold HEPES artificial cerebrospinal fluid (aCSF; in mM, 92 NaCl, 2.5 KCl, 1.2 NaH$_2$PO$_4$, 30 NaHCO$_3$, 20 HEPES, 25 glucose, 5 sodium ascorbate, 2 thiourea, 3 sodium pyruvate, 10 MgSO$_4$, 0.5 CaCl$_2$) bubbled with carbogen gas (95% O$_2$/5% CO$_2$). Slices were recovered at 34°C first in N-methyl-D-Glucamine (NMDG) based recovery solution (in mM, 93 NMDG, 2.5 KCl, 1.2 NaH$_2$PO$_4$, 30 NaHCO$_3$, 20 HEPES, 25 glucose, 5 sodium ascorbate, 2 thiourea, 3 sodium pyruvate, 10 MgSO$_4$, 0.5 CaCl$_2$) for 10–12 min before moving to back to HEPES aCSF. Following 30 min, slices were transferred to recording aCSF (in mM, 124 NaCl, 2.5 KCl, 1.2 NaH$_2$PO$_4$, 24 NaHCO$_3$, 5 HEPES, 12.5 glucose, 2 MgSO$_4$, 2 CaCl$_2$) at room temperature.

Whole-cell recording

Slices were transferred to an open bath recording chamber perfused with aCSF, and visualized with an Olympus BX51WI upright microscope. Intracellular electrodes (4–6 MΩ) were filled with potassium-based recording solution (in mM, 135 K-gluconate, 10 HEPES, 10 Na$_2$-phosphocreatine, 4 KCl, 4 MagATP, 0.3 Na$_2$ATP; pH 7.2). Following whole-cell configuration, pyramidal cells from either CA1 or PC layer II were injected with depolarizing currents from 200 to 300 pA in 20 pA steps to generate a current–voltage (I/O) relationship. AP properties were based on the first recorded AP. The amplitude of AP was measured from resting membrane potential to peak, and half-width was measured as the width at half of the maximum amplitude. The fast AHP was measured as the negative-going peak relative to the AP threshold. The rheobase was defined as the minimum somatic current required to elicit an AP. Input resistance was calculated from the voltage responses to −20 pA current injections. To compare medium and slow AHP, a 100-ms current pulse was injected to generate 4 APs. PC neurons were held at −60 mV and CA1 neurons were held at −55 mV
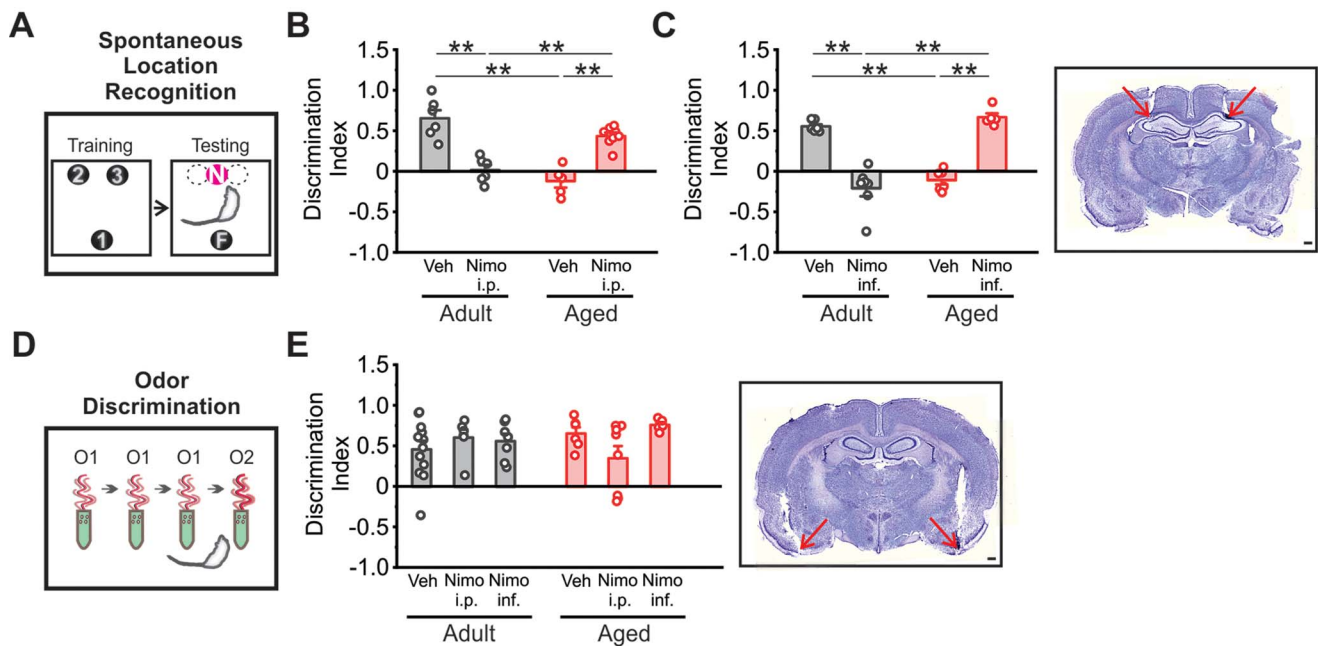
Fig. 1. LTCC blockade has age-dependent effects on spatial discrimination. **A)** Schematics for the spontaneous location recognition task. N: novel object location. F: familial object location. **B)** Nimodipine i.p. injection prevented spatial discrimination learning in adult rats (Veh: $N = 6$; Nimo: $n = 6$), but rescued learning deficiency in aged rats (Veh: $n = 5$; Nimo: $n = 8$). **C)** Nimodipine CA1 infusion blocked spatial discrimination learning in adult rats (Veh: $n = 7$; Nimo: $n = 7$), but rescued learning deficiency in aged rats (Veh: $n = 6$; Nimo: $n = 5$). Right panel shows a Nissl staining example of CA1 targeting. **D)** Schematics for the odor discrimination task. **E)** Nimodipine administration (i.p. or piriform cortex (PC) infusion) did not affect similar odor discrimination in either adult or aged rats. Right panel shows a Nissl staining example of PC targeting. Veh: vehicle. Nimo: nimodipine. Scale bars: 500 μm. **$P < 0.01$.

for AHP recording. AHP area was calculated from where the signal crossed baseline to 1 s following this intersection. Series resistance was ≤ 25 MΩ and experiments were terminated if this range was exceeded. Nimodipine (10 μM; Tocris Bioscience, Bristol, UK) was bath applied during recording. Liquid junction potential was -12 mV and membrane potentials were corrected offline.

Electrophysiological data were recorded with Multiclamp 700B (Molecular Devices, San Jose, CA) filtered at 2 kHz, and digitized at 10 kHz. Data acquisition and analysis were performed with pClamp 10.5 and ClampFit 10.5 (Molecular Devices, San Jose, CA).

Results

LTCCs are required for adult spatial discrimination learning but impair the spatial learning in aged rats

We first explored age-dependent roles of LTCC in 2 behavioral tasks requiring either hippocampal or PC function. In a spatial task that is dependent on hippocampal function (Bekinschtein et al. 2013), rats were trained to distinguish a novel object location from a familiar one (Fig. 1A). There were significant effects of age ($F_{1,21} = 6.247$, $P = 0.021$) and an age × treatment interaction ($F_{1,21} = 70.741$, $P < 0.001$) when nimodipine was injected systemically (Fig. 1B; Supplementary Fig. 2). In adult rats, the vehicle group showed successful spatial location recognition while nimodipine injection prevented object discrimination ($P < 0.001$). In contrast, in aged rats, vehicle rats showed impaired spatial location recognition, which was rescued by nimodipine injection

($P < 0.001$). We then infused nimodipine into the dorsal hippocampal CA1 (100 μM) during the spontaneous object location task (Fig. 1C). There were significant effects of nimodipine on both age groups ($F_{1,21} = 134.615$, $P < 0.001$; Fig. 1C). Nimodipine prevented spatial location recognition in the adult rats ($P < 0.01$). In the aged rats, nimodipine 100-μM infusion rescued the spatial location recognition deficiency ($P < 0.001$).

In the similar odor discrimination task (Fig. 1D), rats were given one odor (O1) 3 times followed by the presentation of another different yet similar odor (O2). The sniffing time difference between the new odor O2 and the familiar odor O1 is an indication of odor discrimination. The LTCC antagonist, nimodipine, either via systemic i.p. injection (5.5 mg/kg), or directly infused to the PC (100 μM), did not affect similar odor discrimination in either adult or aged rats (age: $F_{1,38} = 0.246$, $P = 0.622$; treatment: $F_{2,38} = 1.144$, $P = 0.329$; age × treatment interaction: $F_{2,38} = 2.522$, $P = 0.094$; Fig. 1E; Supplementary Fig. 3).

LTCCs are required for adult odor associative learning but impair the associative learning in aged rats

We then tested the effects of LTCC blockade in an associative learning paradigm that involves the interaction of PC and hippocampus (Zelcer et al. 2006). Rats were trained to associate one of the 2 odors with a food reward (Fig. 2A). The percentage time rats spent nose poking the correct scented sponge containing the retrievable food reward indexes learning progression. During memory tests at various durations following the initial learning,
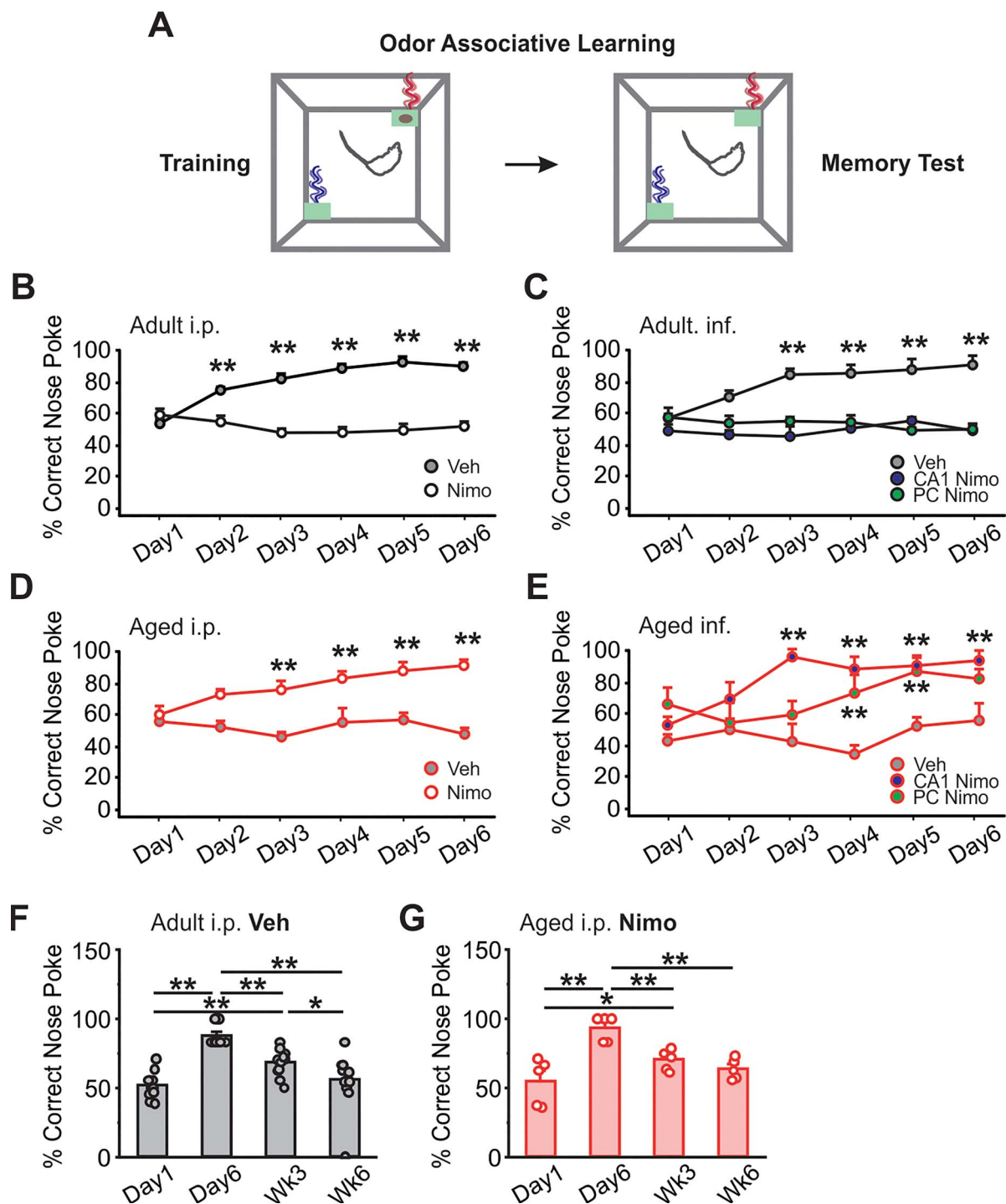
Fig. 2. LTCC blockade has age-dependent effects on olfactory associative learning. **A)** Schematics for the odor associative learning paradigm. **B)** Nimodipine i.p. administration prevented odor associative learning in adult rats (Veh: $n = 11$; Nimo: $n = 6$). **C)** PC ($n = 10$) or hippocampal CA1 infusion ($n = 5$) of nimodipine prevented odor associative learning in adult rats (veh: $n = 11$). **D)** Nimodipine i.p. administration permitted odor associative learning in aged rats (Veh: $n = 6$; Nimo: $n = 6$). **E)** PC ($n = 6$) or hippocampal CA1 infusion ($n = 6$) of nimodipine permitted odor associative learning in aged rats (Veh: $n = 6$). **F)** Memory duration in adult rats with vehicle injection ($n = 11$). **G)** Memory duration in aged rats with nimodipine injection ($n = 5$). *$P < 0.05$, **$P < 0.01$.

rats were exposed to the same 2 scented sponges, without any food reward.

In the adult rats, nimodipine administration either using a systemic injection ($F_{5,75} = 15.418$, $P < 0.001$; Fig. 2B), or a direct infusion into either the PC or CA1 ($F_{10,115} = 4.836$, $P < 0.001$; Fig. 2C) prevented odor associative learning. The vehicle group was pooled from systemic injected and brain infused vehicle rats. Cfos activation following 6 days of odor associative training showed increased cfos+ cells in the PC. However, blocking LTCCs in either the PC or CA1 during the training reduced cfos activation in the PC following
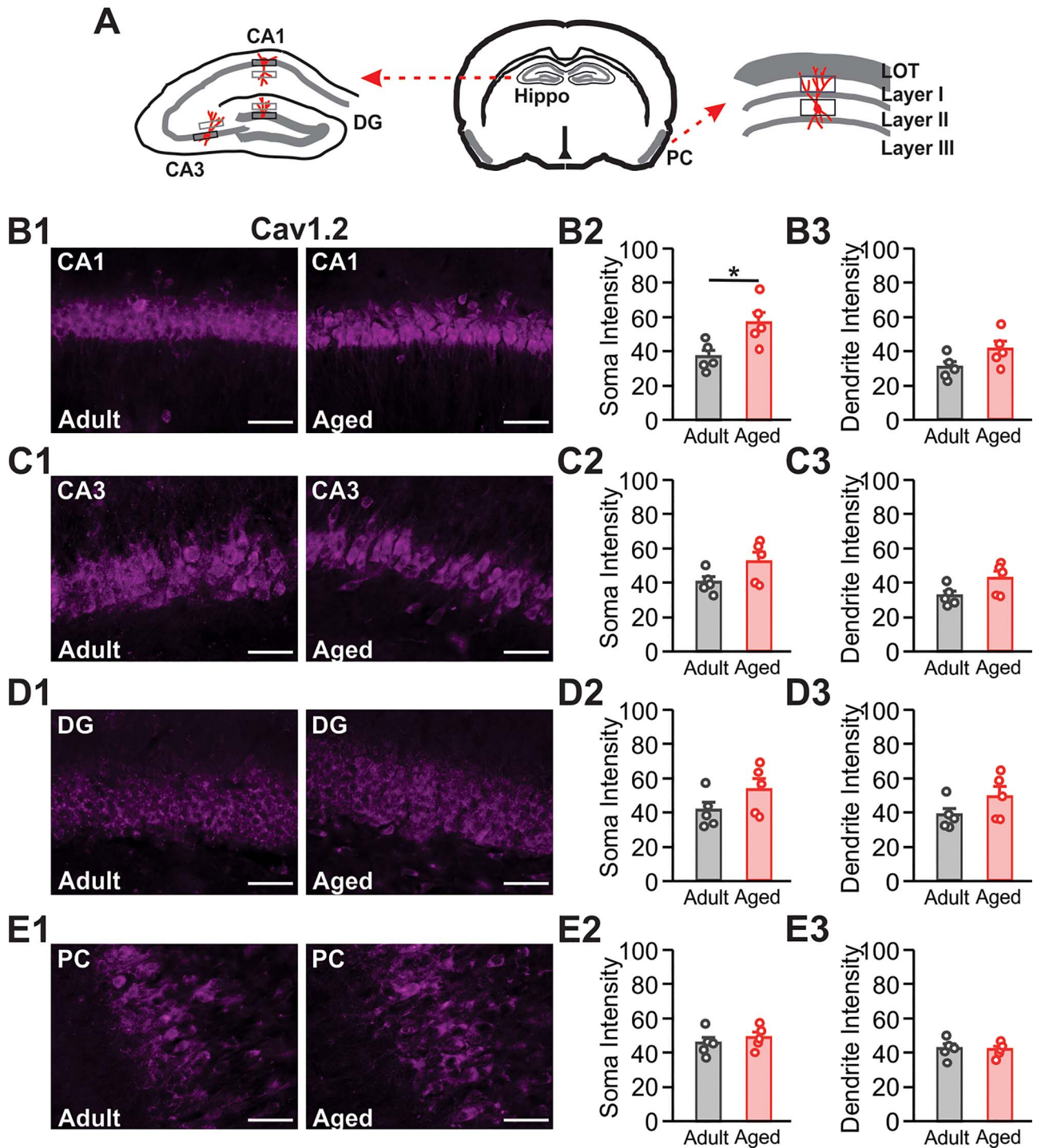
Fig. 3. LTCC Cav1.2 subunit somatic and dendritic expressions in the hippocampus and piriform cortex. **A**) Schematics for regions of interest for LTCC subunit expression measurement. **B1–3**) Cav1.2 expression in the somatic and dendritic layers of the CA1. **C1–3**) Cav1.2 expression in the somatic and dendritic layers of the CA3. **D1–3**) Cav1.2 expression in the somatic and dendritic layers of the DG. **E1–3**) Cav1.2 expression in the somatic and dendritic layers of the PC. Scale bars: 50 μm. $n = 5$, *$P < 0.05$, **$P < 0.01$.

training (Supplementary Fig. 4), consistent with learning prevention induced by nimodipine in either sites.

Intriguingly, in the aged cohort, while vehicle rats did not form odor associative learning during the 6-day training period, nimodipine systemic injection rescued the odor associative learning ($F_{5,45} = 3.679$, $P = 0.007$; Fig. 2D). Similarly, nimodipine brain infusions also rescued learning deficiency in aged rats ($F_{5,60} = 2.401$, $P = 0.018$; Fig. 2E).

PC infused rats appeared to learn the association more slowly than the CA1 infused rats, however (significantly different from the vehicle group ($P < 0.01$) from day 4 in the PC, from day 3 in the CA1 group ($P < 0.01$)).

LTCCs are critically involved in late-phase long-term potentiation (LTP) and long-term memory formation (Moosmang et al. 2005; Mukherjee and Yuan 2016). Here, we assessed whether LTCC blockade affects memory
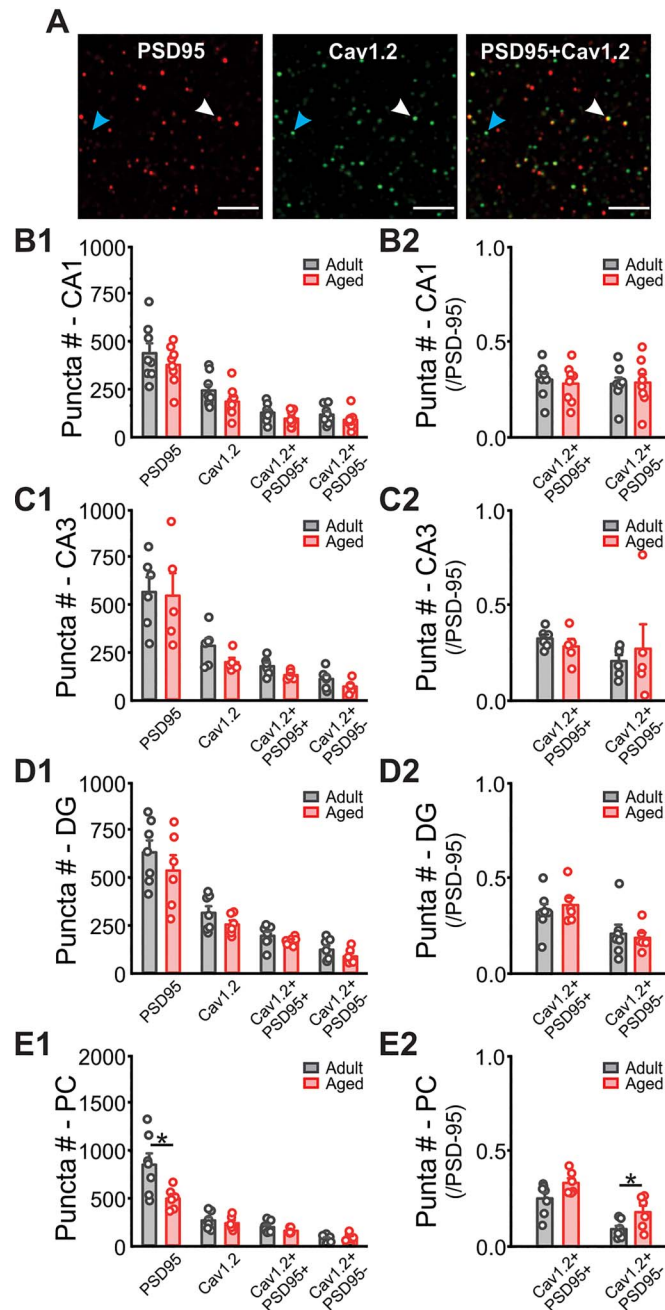
Fig. 4. LTCC Cav1.2 subunit synaptic (PSD95⁺) and extra-synaptic (PSD95⁻) expressions. **A)** Example confocal images of PSD95 (red), Cav1.2 (green) and double labeling (yellow). White arrows: Cav1.2 co-labeled with PSD95. Blue arrows: Cav1.2 not co-labeled with PSD95. **B1–2)** puncta numbers of PSD95, Cav1.2 and co-labeling in the CA1 (adult: $n = 8$; aged: $n = 8$). **C1–2)** puncta numbers of PSD95, Cav1.2 and co-labeling in the CA3 (adult: $n = 6$; aged: $n = 5$). **D1–2)** puncta numbers of PSD95, Cav1.2 and co-labeling in the DG (adult: $n = 7$; aged: $n = 6$). **E1–2)** puncta numbers of PSD95, and Cav1.2 and co-labeling in the PC layer I (adult: $n = 7$; aged: $n = 6$). Scale bars: 5 μm. *$P < 0.05$.

duration. The odor memory duration in adult rats with vehicle injection was compared with that in aged rats whose learning was rescued by nimodipine injection. In both adult ($F_{3,40} = 16.683$, $P < 0.001$; Fig. 2F) and aged rats ($F_{3,13} = 11.124$, $P < 0.001$, Fig. 2G), there is a decline of the associative memory with time. Memories in both adult ($P < 0.01$) and aged rats ($P < 0.05$) lasted for 3 weeks compared with the first day of the training. By 6 weeks, the odor associative memory was lost in both groups ($P > 0.05$ compared with day 1 of the training).

LTCC subunit Cav1.2 expressions are higher in aged hippocampal CA1, but not PC pyramidal neuron somata

The LTCC subunit Cav1.2 is most abundant in the brain (Hell et al. 1993) and a prominent regulator of multiple neuronal functions including excitability and synaptic plasticity. We compared the LTCC subunit Cav1.2 expressions in the hippocampal CA1, CA3, dentate gyrus (DG) and PC pyramidal cell, and dendritic layers (Fig. 3A). There was significantly higher expression of
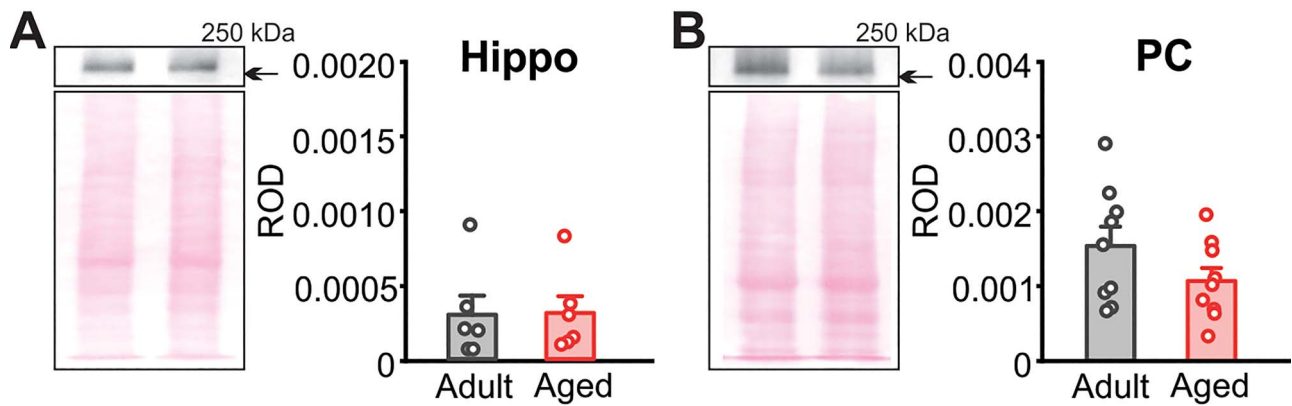
Fig. 5. LTCC Cav1.3 subunit expressions in the hippocampus and piriform cortex. **A**) Cav1.3 expressions in the adult and aged hippocampus (hippo; adult: $n = 6$; aged: $n = 6$). **B**) Cav1.3 expressions in the adult and aged piriform cortex (PC; adult: $n = 9$; aged: $n = 9$). Optical densities of the protein bands were normalized to Ponceau staining of corresponding total protein density. ROD: relative optical density.

Table 1. Intrinsic properties of CA1 neurons.

Intrinsic properties	Adult CA1 neurons ($N = 12$)	Aging CA1 neurons ($N = 11$)
RMP (mV)	-72.77 ± 1.09	-74.91 ± 1.73
Rheobase (pA)	126.67 ± 16.76	138.18 ± 20.08
AP threshold (mV)	-51.54 ± 1.96	$-45.15 \pm 2.33*$
AP amplitude (mV)	109.92 ± 3.22	110.43 ± 5.51
AP half-width (ms)	1.78 ± 0.14	1.69 ± 0.21
fAHP amplitude (mV)	-7.34 ± 0.85	$-13.95 \pm 1.80**$
Input resistance (MΩ)	136.55 ± 9.12	$186.69 \pm 17.86*$

RMP: resting membrane potential; AP: action potential; fAHP: fast afterhyperpolarization. $*P < 0.05$. $**P < 0.01$.

Cav1.2 in the somata ($t = 2.882$, $P = 0.020$) in the aged CA1, but not in the dendritic layer ($t = 1.960$, $P = 0.086$; Fig. 3B1–3). Cav1.2 expressions were not different in the aged CA3 (Somatic: $t = 1.934$, $P = 0.089$; Dendritic: $t = 2.077$, $P = 0.071$; Fig. 3C1–3) and DG (Somatic: $t = 1.571$, $P = 0.155$; Dendritic: $t = 1.555$, $P = 0.159$; Fig. 3D1–3). In the PC, there was no age-dependent difference in Cav1.2 expression in either the somatic ($t = 0.730$, $P = 0.486$) or dendritic layer ($t = 0.220$, $P = 0.831$; Fig. 3E1–3).

Besides somata and dendrites, Cav1.2 is also expressed in dendritic spines (Hell et al. 1993; Davare et al. 2001; Hoogland and Saggau 2004). We analyzed region-specific expressions of Cav1.2 in CA1, CA3, DG, and PC using IHC and confocal imaging in the dendritic layers (Fig. 4). We used co-labeling of the Cav1.2 with PSD95 to index synaptic location of the LTCC (examples see Fig. 4A). Cav1.2 expression profiles showed no significant differences in either synaptic (PSD95+) or extrasynaptic (PSD95−) components between the adult and aged CA1 ($P > 0.05$; Fig. 4B1–2), CA3 ($P > 0.05$; Fig. 4C1–2) and DG ($P > 0.05$; Fig. 4D1–2). In the PC, there was a downregulation of PSD95 with age in layer I ($t = 2.620$, $P = 0.024$) and no difference in overall PSD95+, or PSD95− Cav1.2 expressions ($P > 0.05$; Fig. 4E1). Reduction in PSD95+ with aging is consistent with previous reports (VanGuilder et al. 2010; Sidhu et al. 2016) and implicates reduced number of postsynaptic spines with aging. When normalized to PSD95 puncta number, the Cav1.2 expressed extrasynaptically (PSD95−) showed enhanced expression in the aged PC layer I ($t = 2.412$, $P = 0.034$, Fig. 4E2).

We also compared the Cav1.3 expression profiles in the adult and aged brains using WB of whole cell lysate. Although both Cav1.2 and Cav1.3 are localized in the somata and primary dendrites of neurons, unlike Cav1.2, Cav1.3 is nearly undetectable in the distal dendrites (Hell et al. 1993). Whether Cav1.3 is associated with dendritic spines is not clear. Our results showed that whole cell Cav1.3 expressions in the hippocampus ($t = 0.071$, $P = 0.945$; Fig. 5A) and PC ($t = 1.503$, $P = 0.152$; Fig. 5B) were not different between the adult and aged animals. The lack of a suitable Cav1.3 antibody for IHC precluded detailed subcellular expression studies.

PC pyramidal neurons do not show age-dependent decreased excitability and increased AHP as observed in the hippocampal CA1 neurons

In the aged hippocampal CA1 neurons, decreased excitability is correlated with increased AHP, induced by excessive influx of calcium through LTCCs (Landfield and Pitler 1984; Power et al. 2002). We measured the intrinsic properties, excitability and AHP of PC pyramidal neurons in adult and aged brain, and compared with those of the CA1 neurons.

In the CA1 (Table 1), AP threshold was higher in the aged neurons ($t = 2.111$, $P = 0.047$). Fast AHP ($t = 3.358$, $P = 0.003$) and input resistance ($t = 2.565$, $P = 0.018$) were higher in the aged than the adult brain. In the PC (Table 2), there were no age-dependent differences in AP threshold or fast AHP. However, higher input resistance

Table 2. Intrinsic properties of PC neurons.

Intrinsic properties	Adult PC neurons ($N = 21$)	Aging PC neurons ($N = 29$)
RMP$^\Delta$ (mV)	-60.38 ± 2.63	$-68.89 \pm 1.83*$
Rheobase (pA)	104.76 ± 9.82	93.10 ± 12.72
AP threshold (mV)	-50.17 ± 1.17	-48.70 ± 1.13
AP amplitude (mV)	100.42 ± 2.34	103.07 ± 2.15
AP half-width (ms)	1.61 ± 0.08	1.62 ± 0.05
fAHP amplitude (mV)	-9.18 ± 0.92	-12.20 ± 1.21
Input resistance (MΩ)	173.26 ± 12.71	$222.36 \pm 14.33*$

RMP$^\Delta$: resting membrane potential (adult: $n = 12$; aged: $n = 19$); AP: action potential; fAHP: fast afterhyperpolarization. $*P < 0.05$.

($t = 2.451$, $P = 0.018$) and more hyperpolarized resting membrane potential ($t = 2.745$, $P = 0.010$) were observed in the aged neurons. Increase in input resistance could be a common feature in aging cells and relate to myelin thickening (Peters 2002).

For excitability, we measured I/O curves of the AP numbers against injected currents. Consistent with previous reports (Disterhoft et al. 1996), aged CA1 neurons showed decreased excitability (Fig. 6A). There was an age difference ($F_{1, 315} = 78.571$, $P < 0.001$) and a difference in age × current interaction ($F_{1, 315} = 2.713$, $P < 0.001$). Decreased excitability in aged CA1 neurons was observed in parallel to an increased medium/slow AHP ($t = 3.262$, $P = 0.005$; Fig. 6B). In contrast, in the PC, aged pyramidal cells showed increased excitability with a significant difference in ages ($F_{1, 630} = 18.744$, $P < 0.001$; Fig. 6C). AHPs were not different between the 2 age groups ($t = 0.374$, $P = 0.712$; Fig. 6D). When nimodipine was applied to the recording aCSF, excitability was increased in both adult (treatment effect: $F_{1, 75} = 48.696$, $P < 0.001$; Fig. 6E) and aged neurons (treatment effect: $F_{1, 75} = 6.049$, $P = 0.016$; Fig. 6F). However, the nimodipine effect was more pronounced in the adult neurons when the AP number in the first 200 ms was measured, consistent with reduced latency to the 1st spike in the presence of nimodipine (Supplementary Fig. 5). Nimodipine increased inter-spike intervals between the 1st and 2nd spikes in both adult and aged neurons (Supplementary Fig. 5).

Together, these results suggest that in the PC, increased excitability of aged pyramidal neurons is likely due to increased input resistance, or altered excitatory and inhibitory coupling of LTCCs (Geier et al. 2011). Nimodipine enhanced the excitability more in the adult PC neurons.

Discussion

In this work, we characterized age-dependent expressions of LTCC subunits and neuronal excitability in the PC and hippocampal CA1, in relation to the functional changes in olfactory and spatial learning. We found, consistent with the literature, LTCC expression was higher in the somata of CA1 pyramidal neurons in aged rats, corresponding with increased AHP and decreased neuronal excitability in the aged. Hippocampus-dependent spatial learning was impaired by LTCC blocker nimodipine in

the adult, consistent with the role of LTCCs in synaptic plasticity. However, the same learning was enhanced by nimodipine administration in the aged rats, possibly through a reduction in excess calcium influx via LTCCs and normalization of neuronal excitability. We posit this rebalancing of calcium led to enhancement of synaptic plasticity, and the improvement we observed in aged learning behaviors. In contrast, PC neurons did not show altered AHP with age, and instead exhibited an age-dependent increase in excitability. In an odor associative learning paradigm, which involves both PC and hippocampus, blocking LTCCs in either the PC or the CA1 prevented learning in the adult, and rescued the learning in the aged rats. The relationship between LTCCs, neuronal excitability and their region-dependent roles in age-dependent learning are discussed in the following sections.

Comparison of age-dependent excitability and AHP in the hippocampal CA1 and PC

Age-related alteration of intrinsic neuronal excitability has been extensively studied in the hippocampus (Landfield and Pitler 1984; Power et al. 2002; Disterhoft and Oh 2007; Matthews et al. 2009; Randall et al. 2012). AHP is important for regulating neuronal excitability and is an integral part of neurotransmission and communication (Rizzo et al. 2014). Fast AHP is mediated by voltage-gated BK channels, which can be activated with increases in intracellular calcium (Matthews et al. 2008). Medium and slow AHPs often occur following a burst of APs, and are mediated by calcium-dependent potassium channels (Lima and Marrion 2007; King et al. 2015). Reduced excitability of aging hippocampal CA1 neurons is attributed to increased slow AHP (Landfield and Pitler 1984; Power et al. 2002), activated by excessive calcium currents through LTCCs (Thibault et al. 2001; Lima and Marrion 2007). Our results are consistent with the previous findings. Decreased excitability in aged CA1 neurons was associated with increased slow AHP in these neurons. In addition, higher AP threshold and increased fast AHP amplitude were observed with aging in CA1 neurons, which could also contribute to reduced excitability as well as increased slow AHP in aged CA1 neurons (Power et al. 2002; Matthews et al. 2009; Randall et al. 2012). However, in another report, while decreases in fast AHP are observed following successful learning,
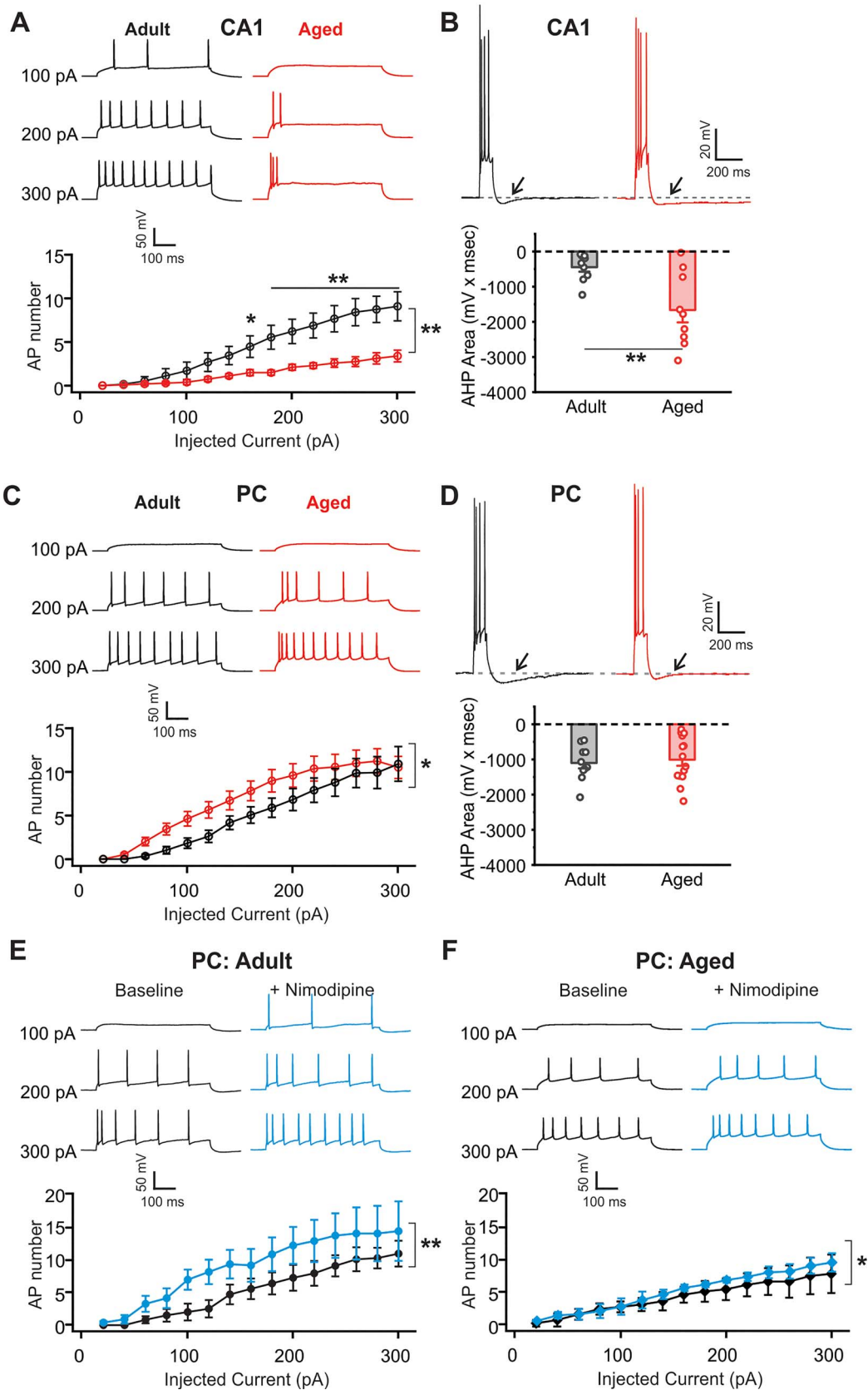
Fig. 6. Age-dependent difference in CA1 and PC neuronal excitability and AHP. **A**) I–O relationship to index neuronal excitability in adult ($n = 12$) and aged CA1 neurons ($n = 11$). **B**) AHP in adult and aged CA1 neurons. **C**) I–O relationship to index neuronal excitability in adult ($n = 17$) and aged PC neurons ($n = 27$). **D**) AHP in adult and aged PC neurons. **E**) Nimodipine increased excitability of adult PC neurons ($n = 6$). **F**) Nimodipine increased excitability of aged PC neurons ($n = 6$). *$P < 0.05$, **$P < 0.01$.

only the slow AHP is observed to increase during aging (Matthews et al. 2008). On the other hand, AP threshold within CA1 neurons of the hippocampus is reported to increase with age but is suspected to be related to alterations of the voltage-gated Na$^+$ channels (Rizzo et al. 2014).

Parallel to a larger AHP in the aged, Cav1.2 were expressed more in aged CA1 somata, consistent with a previous report (Nunez-Santana et al. 2014). An increase in Cav1.2 expression in aged CA3 somata was also reported by Nunez-Santana et al., however, no significant increase of Cav1.2 in aged CA3 was observed here. Conflicting results have been reported regarding aging-associated Cav1.3 expressions, with either increase or decrease, or no change in CA1 or CA3 (Herman et al. 1998; Veng and Browning 2002; Nunez-Santana et al. 2014). Differences in methodology (mRNA vs. protein, IHC vs. WB, subregion dissection vs. whole tissue extraction) and species may account for the different results obtained. The lack of a suitable Cav1.3 antibody for IHC (Nunez-Santana et al. 2014) prevented us from detailed subcellular characterization of Cav1.3.

Our results in rat PC neurons show a striking contrast to CA1 neurons. Aged PC neurons showed a small but significant increase in excitability, whereas neither slow nor fast AHPs were different between the age groups. The increase in aged PC neuronal excitability may be related to the increased membrane input resistance observed in these neurons, or difference in LTCC coupling to downstream effectors. Cav1.2 and Cav1.3 couple to different Ca^{2+}-dependent conductance. The hyperpolarizing-dependent AHP is mediated by Cav1.3 and Cav1.2 (Liebmann et al. 2008; Hasreiter et al. 2014; Sahu et al. 2017). An excitatory conductance (afterdepolarization, ADP), on the other hand, is mediated solely by Cav1.2 and increases neuronal excitability (Hasreiter et al. 2014). LTCC Cav1.2 expressions were similar in the somata of adult and aged PC. However, there was a relative higher number of extrasynaptic puncta to PSD95 in aged PC. Cav1.3 whole-cell expressions were also similar in adult and aged PCs. Aging may impact the typical coupling pathways of Cav1.2 and Cav1.3 to excitatory and inhibitory conductance, respectively, even though we did not observe a difference in AHP in the 2 age groups.

Age-dependent roles of LTCCs in spatial and olfactory learning

LTCCs can influence learning in 2 ways: altering excitability via AHP and ADP and indirectly affecting LTP threshold, or directly affecting LTP/long-term depression (LTD) by coupling calcium with intracellular plasticity machinery (Impey et al. 1996; Deisseroth et al. 1998; Rajadhyaksha et al. 1999; Ma et al. 2014; Rajani et al. 2021).

In adult rats, blocking LTCC function by nimodipine infusion in the CA1, prevented novel location recognition, consistent with its role in spatial memory and hippocampal LTP. On the other hand, LTCC blockade in the PC

did not affect difficult odor discrimination, suggesting LTCCs do not affect basal synaptic transmission and odor perception in PC. However, in the odor associative learning paradigm, nimodipine infusion in either the PC, or the CA1, prevented the development of odor associative learning, as well as the cfos activation in the PC associated with the conditioned odor. This is consistent with previous reports that odor associative learning involves both hippocampal and PC functions (Truchet et al. 2002; Zelcer et al. 2006; Rangel et al. 2016).

The PC and hippocampus share extensive mutual connections. CA1 axons directly project to the PC (Cenquizca and Swanson 2007). The PC sends substantial efferent inputs to the hippocampus via lateral entorhinal cortex (Kerr et al. 2007). Recently, patterned stimulation of the PC was shown to evoke excitatory potentials and trigger LTP in the hippocampal DG (Strauch and Manahan-Vaughan 2020). Odor associative learning modifies synaptic efficiency in both hippocampus and PC (Truchet et al. 2002). An early potentiation of the hippocampal DG occurs when rats start to discriminate the odor cues, whereas a PC LTP-like potentiation is observed in the later sessions (3–5 days) when rats have perfectly mastered the sessions (Truchet et al. 2002). In a similar odor associative learning model (Zelcer et al. 2006), rule learning is accompanied by a transient global increase in CA1 neuronal excitability, followed by a long-lasting synaptic potentiation in the PC. These studies suggest that the hippocampus initiates the encoding of converging cues and supports the development of PC plasticity and memory retrieval.

In the aged rats, both CA1 and PC nimodipine infusions permitted odor associative learning, which did not occur in vehicle-infused aged rats. Aging-associated increased expression of LTCCs in CA1, increased AHP and decreased excitability in CA1 neurons observed by us and others likely explain the failure of the odor associative learning as well as the spatial learning in the aged rats. Nimodipine could permit associative learning by blocking LTCCs, normalizing calcium influx, reducing AHP, and restoring CA1 neuronal excitability. However, direct effects of nimodipine on other voltage-dependent potassium channels (Zhang and Gold 2009) cannot be excluded. Nimodipine also has cerebral vasodilation effects (Scriabine and van den Kerckhoff 1988) which may also contribute to enhanced cerebral blood flow and cognitive function. Nevertheless, this does not explain the opposite effects of nimodipine in adult vs. aged animals.

It is intriguing, however, that PC nimodipine infusion also enhanced learning in the aged animals. The rescue of learning is not likely associated with normalization of PC neuronal excitability as may have occurred in the aged CA1 neurons. Aged PC showed higher excitability compared with adult PC. Nimodipine application enhanced excitability of PC neurons. We suspect nimodipine may directly influence synaptic plasticity in the aged PC by acting at extrasynaptic

Cav1.2 (PSD95⁻) channels. Relative higher amounts of these channels in relation to the PSD95 numbers may favor "LTD"-like processes and increase the threshold for learning. Indeed, a shift from NMDAR-dependent to LTCC-dependent LTD has been recently reported in the PC layer Ib associational fibers with aging (Rajani et al. 2021). Alternately, LTCCs could generate desynchronization between PC and hippocampal cells in the aged animals and prevent synaptic plasticity, which merits future investigation.

Conclusion

Our study provides the first evidence of aging-associated changes in neuronal properties of the PC. Unlike aged CA1 neurons, aged PC neurons do not show LTCC somatic overexpression or neuronal hypoexcitability. However, dysfunction of LTCCs does exist in the PC with aging and affects olfactory plasticity and learning. This suggests that aging differentially modulate LTCC functions in the 2 structures. The hippocampus is the encoding site for new episodic memories in both human and animals. It also initiates and synchronizes cue retrieval during memory recall (Manns et al. 2007a, 2007b; Strauch and Manahan-Vaughan 2020). Therefore, the excitability changes in hippocampal CA1 may have broad influences on memory coding sites in the brain. In fact, a transient increase of CA1 neuronal excitability following odor discrimination rule learning facilitates the learning of other spatial tasks (Zelcer et al. 2006). On the other hand, cortical structures for longer memory storage, such as the PC studied here, may be more stable and less prone to age-related excitability changes.

Acknowledgements

Supplementary material

Supplementary material can be found at *Cerebral Cortex* online.

Funding

References

Ban TA, Morey L, Aguglia E, Azzarelli O, Balsano F, Marigliano V, Caglieris N, Sterlicchio M, Capurso A, Tomasi NA, et al. Nimodipine in the treatment of old age dementias. *Prog Neuro-Psychopharmacol Biol Psychiatry*. 1990:14:525–551.

Barkai E, Saar D. Cellular correlates of olfactory learning in the rat piriform cortex. *Rev Neurosci*. 2001:12:111–120.

Batuecas A, Pereira R, Centeno C, Pulido JA, Hernandez M, Bollati A, Bogonez E, Satrustegui J. Effects of chronic nimodipine on working memory of old rats in relation to defects in synaptosomal calcium homeostasis. *Eur J Pharmacol*. 1998:350:141–150.

Bekinschtein P, Kent BA, Oomen CA, Clemenson GD, Gage FH, Saksida LM, Bussey TJ. BDNF in the dentate gyrus is required for consolidation of "pattern-separated" memories. *Cell Rep*. 2013:5: 759–768.

Buonarati OR, Henderson PB, Murphy GG, Horne MC, Hell JW. Proteolytic processing of the L-type Ca (2+) channel alpha 11.2 subunit in neurons. *F1000Res*. 2017:6:1166.

Campbell LW, Hao SY, Thibault O, Blalock EM, Landfield PW. Aging changes in voltage-gated calcium currents in hippocampal CA1 neurons. *J Neurosci*. 1996:16:6286–6295.

Cenquizca LA, Swanson LW. Spatial organization of direct hippocampal field CA1 axonal projections to the rest of the cerebral cortex. *Brain Res Rev*. 2007:56:1–26.

Chakrabarti A, Saini HK, Garg SK. Dose-finding study with nimodipine: a selective central nervous system calcium channel blocker on aminophylline induced seizure models in rats. *Brain Res Bull*. 1998:45:495–499.

Davare MA, Hell JW. Increased phosphorylation of the neuronal L-type Ca(2+) channel Ca(v)1.2 during aging. *Proc Natl Acad Sci U S A*. 2003:100:16018–16023.

Davare MA, Avdonin V, Hall DD, Peden EM, Burette A, Weinberg RJ, Horne MC, Hoshi T, Hell JW. A beta2 adrenergic receptor signaling complex assembled with the Ca2+ channel Cav1.2. *Science*. 2001:293:98–101.

Deisseroth K, Heist EK, Tsien RW. Translocation of calmodulin to the nucleus supports CREB phosphorylation in hippocampal neurons. *Nature*. 1998:392:198–202.

Deyo RA, Straube KT, Disterhoft JF. Nimodipine facilitates associative learning in aging rabbits. *Science*. 1989:243:809–811.

Disterhoft JF, Oh MM. Alterations in intrinsic neuronal excitability during normal aging. *Aging Cell*. 2007:6:327–336.

Disterhoft JF, Thompson LT, Moyer JR Jr, Mogul DJ. Calcium-dependent afterhyperpolarization and learning in young and aging hippocampus. *Life Sci*. 1996:59:413–420.

Disterhoft JF, Wu WW, Ohno M. Biophysical alterations of hippocampal pyramidal neurons in learning, ageing and Alzheimer's disease. *Ageing Res Rev*. 2004:3:383–406.

Eichenbaum H, Robitsek RJ. Olfactory memory: a bridge between humans and animals in models of cognitive aging. *Ann N Y Acad Sci*. 2009:1170:658–663.

Geier P, Lagler M, Boehm S, Kubista H. Dynamic interplay of excitatory and inhibitory coupling modes of neuronal L-type calcium channels. *Am J Physiol Cell Physiol*. 2011:300:C937–C949.

Ghosh A, Carew SJ, Chen X, Yuan Q. The role of L-type calcium channels in olfactory learning and its modulation by norepinephrine. *Front Cell Neurosci*. 2017a:11:394.

Ghosh A, Mukherjee B, Chen X, Yuan Q. Beta-Adrenoceptor activation enhances L-type calcium channel currents in anterior piriform cortex pyramidal cells of neonatal mice: implication for odor learning. *Learn Mem*. 2017b:24: 132–135.

Ghosh A, Torraville SE, Mukherjee B, Walling SG, Martin GM, Harley CW, Yuan Q. An experimental model of Braak's pretangle proposal for the origin of Alzheimer's disease: the role of locus coeruleus in early symptom development. *Alzheimers Res Ther*. 2019:11:59.

Hasreiter J, Goldnagl L, Bohm S, Kubista H. Cav1.2 and Cav1.3 L-type calcium channels operate in a similar voltage range but show different coupling to ca(2+)-dependent conductances in hippocampal neurons. *Am J Physiol Cell Physiol*. 2014:306: C1200–C1213.

Hell JW, Westenbroek RE, Warner C, Ahlijanian MK, Prystay W, Gilbert MM, Snutch TP, Catterall WA. Identification and differential subcellular localization of the neuronal class C and class D L-type calcium channel alpha 1 subunits. *J Cell Biol*. 1993:123: 949–962.

Herman JP, Chen KC, Booze R, Landfield PW. Up-regulation of alpha1D Ca2+ channel subunit mRNA expression in the hippocampus of aged F344 rats. *Neurobiol Aging*. 1998:19: 581–587.

Hoogland TM, Saggau P. Facilitation of L-type Ca2+ channels in dendritic spines by activation of beta2 adrenergic receptors. *J Neurosci*. 2004:24:8416–8427.

Hopp SC, D'Angelo HM, Royer SE, Kaercher RM, Adzovic L, Wenk GL. Differential rescue of spatial memory deficits in aged rats by L-type voltage-dependent calcium channel and ryanodine receptor antagonism. *Neuroscience*. 2014:280:10–18.

Impey S, Mark M, Villacres EC, Poser S, Chavkin C, Storm DR. Induction of CRE-mediated gene expression by stimuli that generate long-lasting LTP in area CA1 of the hippocampus. *Neuron*. 1996:16: 973–982.

Kerr KM, Agster KL, Furtak SC, Burwell RD. Functional neuroanatomy of the parahippocampal region: the lateral and medial entorhinal areas. *Hippocampus*. 2007:17:697–708.

Khachaturian ZS. Towards theories of brain aging. In: DWK K, Burrows GD, editors. *Handbook of studies on psychiatry and old age New York*. Amsterdam: Elsevier; 1984. pp. 7–30

Khachaturian ZS. The role of calcium regulation in brain aging: reexamination of a hypothesis. *Aging (Milano)*. 1989:1:17–34.

King B, Rizwan AP, Asmara H, Heath NC, Engbers JD, Dykstra S, Bartoletti TM, Hameed S, Zamponi GW, Turner RW. IKCa channels are a critical determinant of the slow AHP in CA1 pyramidal neurons. *Cell Rep*. 2015:11:175–182.

Landfield PW. 'Increased calcium-current' hypothesis of brain aging. *Neurobiol Aging*. 1987:8:346–347.

Landfield PW, Pitler TA. Prolonged Ca2+−dependent afterhyperpolarizations in hippocampal neurons of aged rats. *Science*. 1984:226: 1089–1092.

Levere TE, Walker A. Old age and cognition: enhancement of recent memory in aged rats by the calcium channel blocker nimodipine. *Neurobiol Aging*. 1992:13:63–66.

Li W, Howard JD, Gottfried JA. Disruption of odour quality coding in piriform cortex mediates olfactory deficits in Alzheimer's disease. *Brain*. 2010:133:2714–2726.

Liebmann L, Karst H, Sidiropoulou K, van Gemert N, Meijer OC, Poirazi P, Joels M. Differential effects of corticosterone on the slow afterhyperpolarization in the basolateral amygdala and CA1 region: possible role of calcium channel subunits. *J Neurophysiol*. 2008:99:958–968.

Lima PA, Marrion NV. Mechanisms underlying activation of the slow AHP in rat hippocampal neurons. *Brain Res*. 2007:1150:74–82.

Lopez-Arrieta JM, Birks J. Nimodipine for primary degenerative, mixed and vascular dementia. *Cochrane Database Syst Rev*. 2002:CD000147.

Ma H, Groth RD, Cohen SM, Emery JF, Li B, Hoedt E, Zhang G, Neubert TA, Tsien RW. gammaCaMKII shuttles Ca(2)(+)/CaM to the nucleus to trigger CREB phosphorylation and gene expression. *Cell*. 2014:159:281–294.

Manns JR, Howard MW, Eichenbaum H. Gradual changes in hippocampal activity support remembering the order of events. *Neuron*. 2007a:56:530–540.

Manns JR, Zilli EA, Ong KC, Hasselmo ME, Eichenbaum H. Hippocampal CA1 spiking during encoding and retrieval: relation to theta phase. *Neurobiol Learn Mem*. 2007b:87:9–20.

Matthews EA, Weible AP, Shah S, Disterhoft JF. The BK-mediated fAHP is modulated by learning a hippocampus-dependent task. *Proc Natl Acad Sci U S A*. 2008:105:15154–15159.

Matthews EA, Linardakis JM, Disterhoft JF. The fast and slow afterhyperpolarizations are differentially modulated in hippocampal neurons by aging and learning. *J Neurosci*. 2009:29:4750–4755.

Michaluk J, Karolewicz B, Antkiewicz-Michaluk L, Vetulani J. Effects of various Ca2+ channel antagonists on morphine analgesia, tolerance and dependence, and on blood pressure in the rat. *Eur J Pharmacol*. 1998:352:189–197.

Moosmang S, Haider N, Klugbauer N, Adelsberger H, Langwieser N, Muller J, Stiess M, Marais E, Schulla V, Lacinova L, et al. Role of hippocampal Cav1.2 Ca2+ channels in NMDA receptor-independent synaptic plasticity and spatial memory. *J Neurosci*. 2005:25:9883–9892.

Moyer JR Jr, Thompson LT, Black JP, Disterhoft JF. Nimodipine increases excitability of rabbit CA1 pyramidal neurons in an age- and concentration-dependent manner. *J Neurophysiol*. 1992:68: 2100–2109.

Mukherjee B, Yuan Q. NMDA receptors in mouse anterior piriform cortex initialize early odor preference learning and L-type calcium channels engage for long-term memory. *Sci Rep*. 2016:6:35256.

Murphy C. Loss of olfactory function in dementing disease. *Physiol Behav*. 1999:66:177–182.

Nunez-Santana FL, Oh MM, Antion MD, Lee A, Hell JW, Disterhoft JF. Surface L-type Ca2+ channel expression levels are increased in aged hippocampus. *Aging Cell*. 2014:13:111–120.

Peters A. The effects of normal aging on myelin and nerve fibers: a review. *J Neurocytol*. 2002:31:581–593.

Poo C, Agarwal G, Bonacchi N, Mainen ZF. Spatial maps in piriform cortex during olfactory navigation. *Nature*. 2021.

Porter NM, Thibault O, Thibault V, Chen KC, Landfield PW. Calcium channel density and hippocampal cell death with age in long-term culture. *J Neurosci*. 1997:17:5629–5639.

Power JM, Wu WW, Sametsky E, Oh MM, Disterhoft JF. Age-related enhancement of the slow outward calcium-activated potassium current in hippocampal CA1 pyramidal neurons in vitro. *J Neurosci*. 2002:22:7234–7243.

Rajadhyaksha A, Barczak A, Macias W, Leveque JC, Lewis SE, Konradi C. L-type Ca(2+) channels are essential for glutamate-mediated CREB phosphorylation and c-fos gene expression in striatal neurons. *J Neurosci*. 1999:19:6348–6359.

Rajani V, Maziar A, Man KNM, Hell JW, Yuan Q. Age-dependent contributions of NMDA receptors and L-type calcium channels to long-term depression in the piriform cortex. *Int J Mol Sci*. 2021:22.

Randall AD, Booth C, Brown JT. Age-related changes to Na+ channel gating contribute to modified intrinsic neuronal excitability. *Neurobiol Aging*. 2012:33:2715–2720.

Rangel LM, Rueckemann JW, Riviere PD, Keefe KR, Porter BS, Heimbuch IS, Budlong CH, Eichenbaum H. Rhythmic coordination of hippocampal neurons during associative memory processing. *Elife*. 2016:5:e09849.

Rizzo V, Richman J, Puthanveettil SV. Dissecting mechanisms of brain aging by studying the intrinsic excitability of neurons. *Front Aging Neurosci*. 2014:6:337.

Ross JM, Fletcher ML. Aversive learning-induced plasticity throughout the adult mammalian olfactory system: insights across development. *J Bioenerg Biomembr*. 2019:51:15–27.

Sahu G, Asmara H, Zhang FX, Zamponi GW, Turner RW. Activity-dependent facilitation of CaV1.3 calcium channels promotes KCa3.1 activation in hippocampal neurons. *J Neurosci*. 2017:37: 11255–11270.

Sandin M, Jasmin S, Levere TE. Aging and cognition: facilitation of recent memory in aged nonhuman primates by nimodipine. *Neurobiol Aging*. 1990:11:573–575.

Scriabine A, van den Kerckhoff W. Pharmacology of nimodipine. A review. *Ann N Y Acad Sci*. 1988:522:698–706.

Sidhu VK, Huang BX, Desai A, Kevala K, Kim HY. Role of DHA in aging-related changes in mouse brain synaptic plasma membrane proteome. *Neurobiol Aging*. 2016:41:73–85.

Strauch C, Manahan-Vaughan D. Orchestration of hippocampal information encoding by the piriform cortex. *Cereb Cortex*. 2020:30:135–147.

Sze KH, Sim TC, Wong E, Cheng S, Woo J. Effect of nimodipine on memory after cerebral infarction. *Acta Neurol Scand*. 1998:97: 386–392.

Thibault O, Landfield PW. Increase in single L-type calcium channels in hippocampal neurons during aging. *Science*. 1996:272: 1017–1020.

Thibault O, Hadley R, Landfield PW. Elevated postsynaptic [Ca2+]i and L-type calcium channel activity in aged hippocampal neurons: relationship to impaired synaptic plasticity. *J Neurosci*. 2001:21:9744–9756.

Thompson LT, Deyo RA, Disterhoft JF. Nimodipine enhances spontaneous activity of hippocampal pyramidal neurons in aging rabbits at a dose that facilitates associative learning. *Brain Res*. 1990:535:119–130.

Tollefson GD. Short-term effects of the calcium channel blocker nimodipine (Bay-e-9736) in the management of primary degenerative dementia. *Biol Psychiatry*. 1990:27: 1133–1142.

Truchet B, Chaillan FA, Soumireu-Mourat B, Roman FS. Learning and memory of cue-reward association meaning by modifications of synaptic efficacy in dentate gyrus and piriform cortex. *Hippocampus*. 2002:12:600–608.

VanGuilder HD, Yan H, Farley JA, Sonntag WE, Freeman WM. Aging alters the expression of neurotransmission-regulating proteins in the hippocampal synaptoproteome. *J Neurochem*. 2010:113: 1577–1588.

Veng LM, Browning MD. Regionally selective alterations in expression of the alpha(1D) subunit (Ca(v)1.3) of L-type calcium channels in the hippocampus of aged rats. *Brain Res Mol Brain Res*. 2002:107: 120–127.

Veng LM, Mesches MH, Browning MD. Age-related working memory impairment is correlated with increases in the L-type calcium channel protein alpha1D (Cav1.3) in area CA1 of the hippocampus and both are ameliorated by chronic nimodipine treatment. *Brain Res Mol Brain Res*. 2003:110:193–202.

Wang W, Wang LN, Zhang XH, Ma L, Li DJ. A nimodipine interventional study of patients with mild cognitive impairment. *Zhonghua Nei Ke Za Zhi*. 2006:45:274–276.

Wesson DW, Borkowski AH, Landreth GE, Nixon RA, Levy E, Wilson DA. Sensory network dysfunction, behavioral impairments, and their reversibility in an Alzheimer's beta-amyloidosis mouse model. *J Neurosci*. 2011a:31:15962–15971.

Wesson DW, Nixon RA, Levy E, Wilson DA. Mechanisms of neural and behavioral dysfunction in Alzheimer's disease. *Mol Neurobiol*. 2011b:43:163–179.

Wilson DA, Sullivan RM. Cortical processing of odor objects. *Neuron*. 2011:72:506–519.

Wilson RS, Arnold SE, Schneider JA, Boyle PA, Buchman AS, Bennett DA. Olfactory impairment in presymptomatic Alzheimer's disease. *Ann N Y Acad Sci*. 2009:1170:730–735.

Wilson DA, Xu W, Sadrian B, Courtiol E, Cohen Y, Barnes DC. Cortical odor processing in health and disease. *Prog Brain Res*. 2014:208: 275–305.

Woodruff-Pak DS, Chi J, Li YT, Pak MH, Fanelli RJ. Nimodipine ameliorates impaired eyeblink classical conditioning in older rabbits in the long-delay paradigm. *Neurobiol Aging*. 1997:18:641–649.

Xu W, Lopez-Guzman M, Schoen C, Fitzgerald S, Lauer SL, Nixon RA, Levy E, Wilson DA. Spared piriform cortical single-unit odor processing and odor discrimination in the Tg2576 mouse model of Alzheimer's disease. *PLoS One*. 2014:9:e106431.

Zanos P, Bhat S, Terrillion CE, Smith RJ, Tonelli LH, Gould TD. Sex-dependent modulation of age-related cognitive decline by the L-type calcium channel gene Cacna1c (Cav 1.2). *Eur J Neurosci*. 2015:42:2499–2507.

Zelcer I, Cohen H, Richter-Levin G, Lebiosn T, Grossberger T, Barkai E. A cellular correlate of learning-induced metaplasticity in the hippocampus. *Cereb Cortex*. 2006:16:460–468.

Zhang XL, Gold MS. Dihydropyridine block of voltage-dependent K+ currents in rat dorsal root ganglion neurons. *Neuroscience*. 2009:161:184–194.

Zhang S, Manahan-Vaughan D. Spatial olfactory learning contributes to place field formation in the hippocampus. *Cereb Cortex*. 2015:25:423–432.